NON-CONTACTING FINGER SEAL DEVELOPMENTS AND DESIGN CONSIDERATIONS

M. Jack Braun, Hazel M. Pierson, Dingeng Deng, and Fred K. Choy
University of Akron
Akron, Ohio

Margaret P. Proctor
National Aeronautics and Space Administration
Glenn Research Center
Cleveland, Ohio

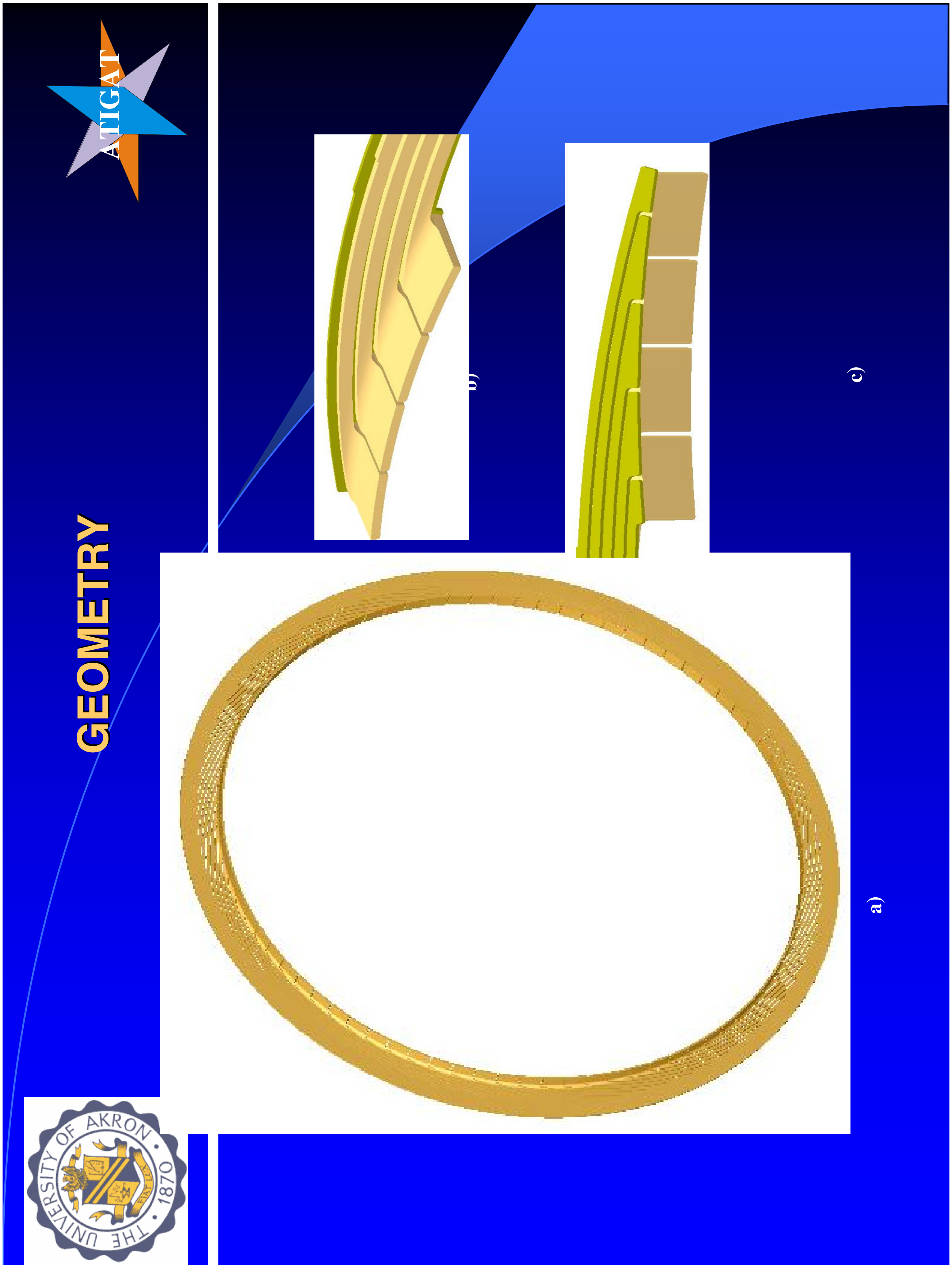

ATIGAT
GEOMETRY
a)
b)
c)

GEOMETRY (cont'd)

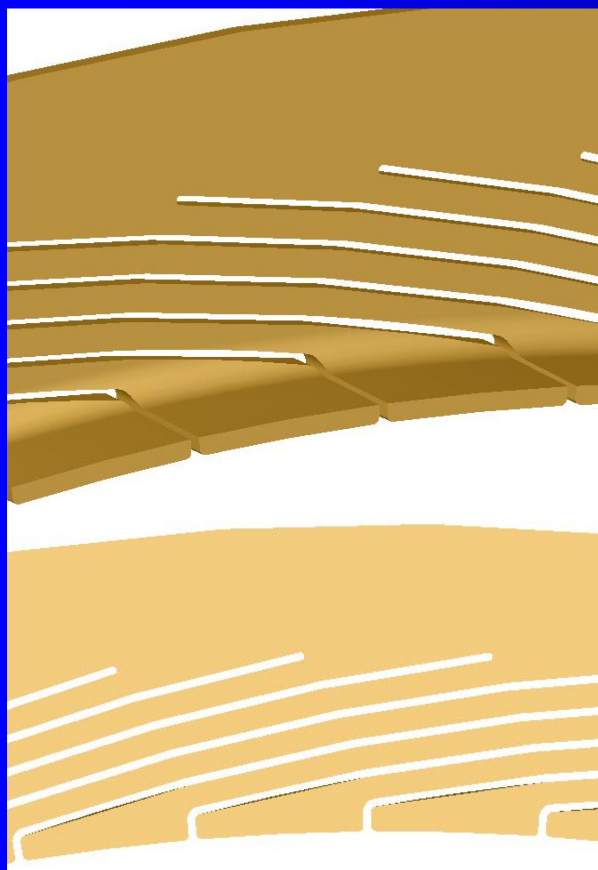

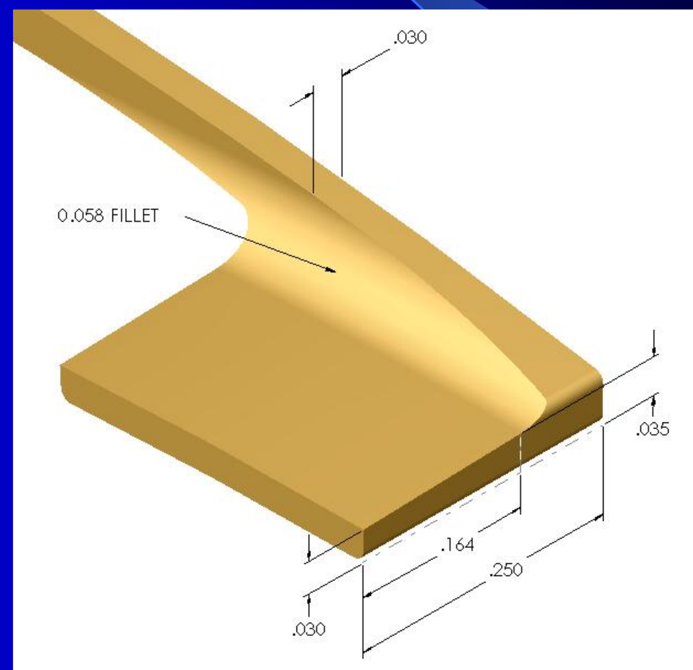

c)

UNDERSTANDING BOUNDARY CONDITIONS

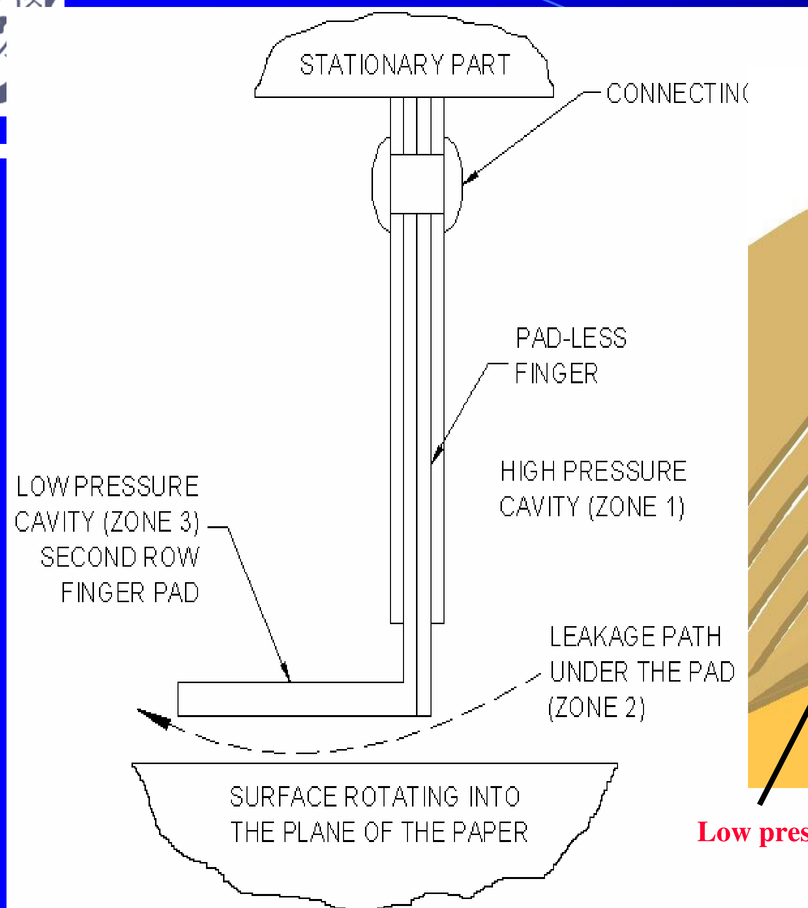

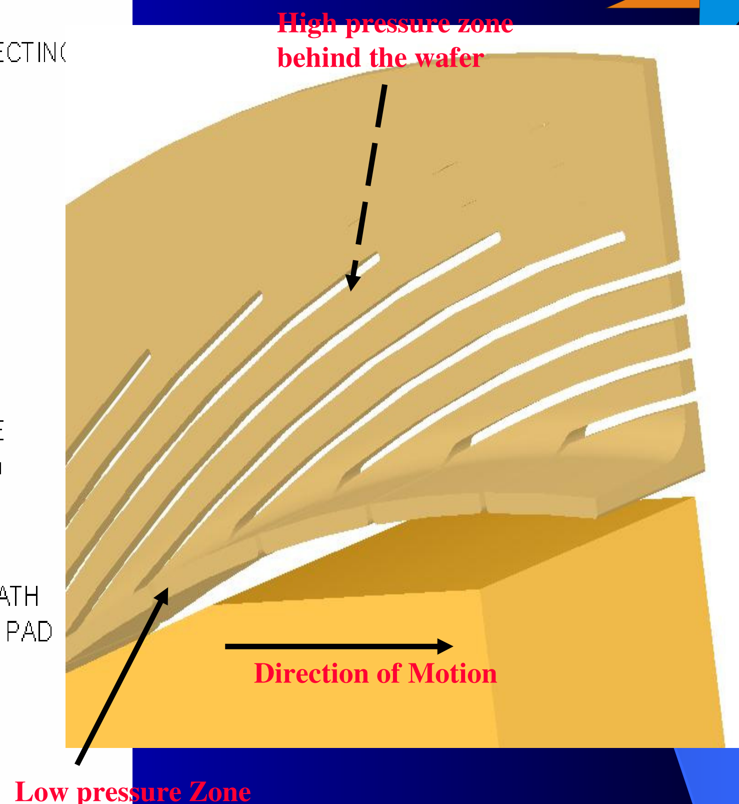

Boundary conditions for the Finger Seal.

Schematic Cross Section with Two Rows of Padded Low- and Pad-less High Pressure Fingers and definition of the pressure zones

Solid model showing the high and low pressure zones

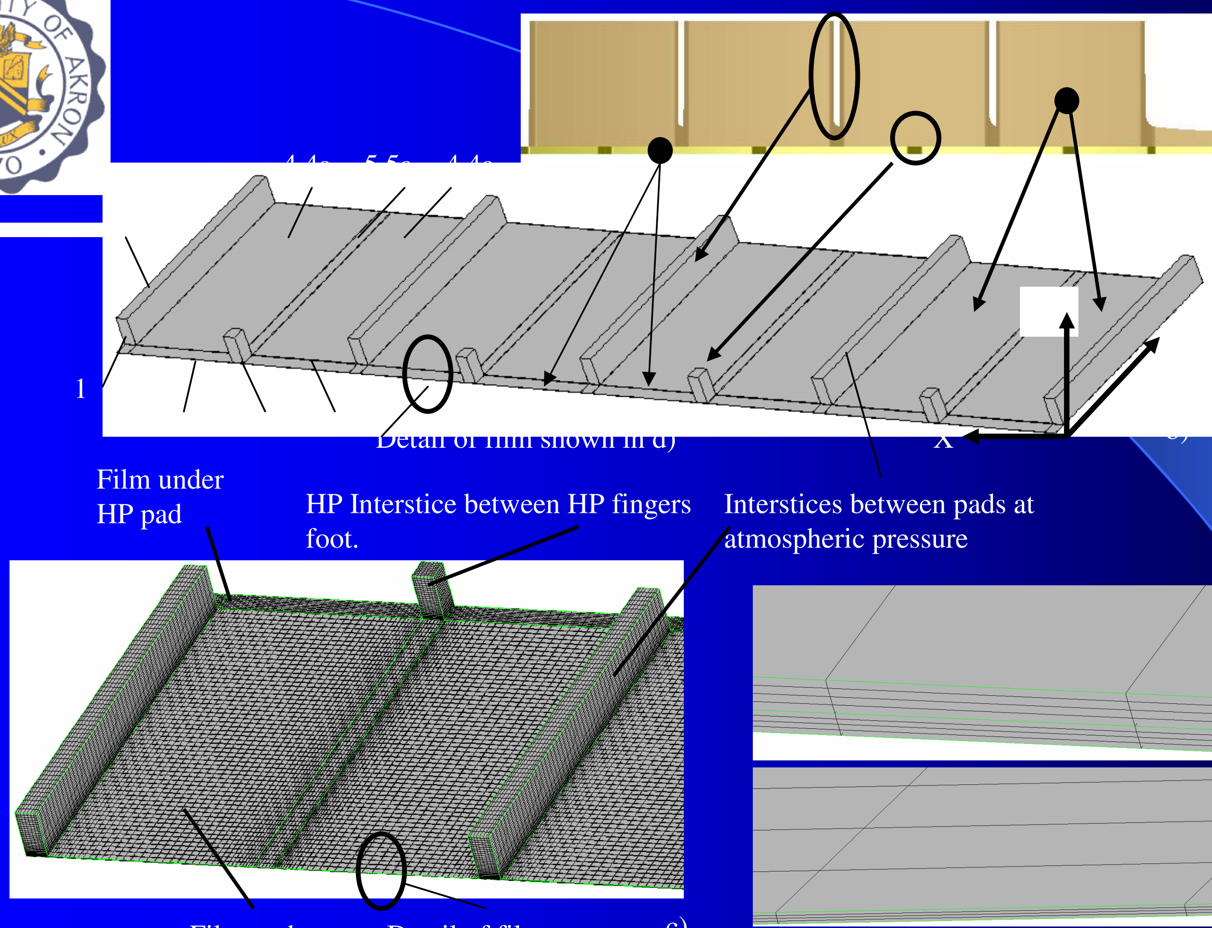

Grid Details for the Pressure, Flow and Temperature Calculations.
a) Solid representation of the two rows of fingers viewed from below
b) Corresponding representation of the fluid film contained between the rotor and the assembly of fingers.
c) Detail of the cell structure in the fluid film below and in-between HP and LP pads.
d) Fluid film grid structure under the HP finger
e) Fluid film grid structure under the LP finger

BLOCK GRIDDING DETAILS AND BOUNDARY CONDITIONS

ATIGAT

Label No.	Number of cells	Remarks	Boundary condition type
1	324	Single block of film between the rotor and the HP finger pad-less foot	Solid wall, top; Rotating wall, bottom
2, 3	17523	Top block of the film, in-between the LP pads	Solid walls, top Interface, bottom
	2124	Bottom block of the film, in-between the LP pads, directly above the rotor; 2 and 3 are contiguous	Outlet, side, LP; Interface, top Rotating wall, bottom
4,4a	9204	Top block of the film, directly under the LP pad	Solid wall, top Interface, bottom
	9204	Bottom block of the film, directly above the rotor; 4 and 4a are contiguous	Interface, top; Rotating wall, bottom
5,5a	2124	Top block of the film, in-between the LP pads	Solid wall, top Interface, bottom
	2124	Bottom block of the film, in-between the LP pads, directly above the rotor, 5a is contiguous with 5	Interface, top Rotating wall, bottom
6,7,8	2349	Top block of the film, in-between the HP fingers' feet	Solid wall, top Interface, bottom
	324	Middle block of the film, in-between the HP fingers' feet	Interface, top Interface, bottom
	324	Bottom block of the film, in-between the HP fingers' feet, directly above the rotor 6,7 and 8 are contiguous between themselves	Interface, top Rotating wall, bottom
9	1404	Single block of film between the rotor and the HP finger pad-less foot	Solid wall top, Rotating wall bottom

BLOCK GRIDDING DETAILS AND BOUNDARY CONDITIONS

ATIGAT

Label No.	Number of cells	Remarks	Boundary condition type
1	324	Single block of film between the rotor and the HP finger pad-less foot	Solid wall, top; Rotating wall, bottom
2, 3	17523	Top block of the film, in-between the LP pads	Solid walls, top Interface, bottom
	2124	Bottom block of the film, in-between the LP pads, directly above the rotor; 2 and 3 are contiguous	Outlet, side, LP; Interface, top Rotating wall, bottom
4,4a	9204	Top block of the film, directly under the LP pad	Solid wall, top Interface, bottom
	9204	Bottom block of the film, directly above the rotor; 4 and 4a are contiguous	Interface, top; Rotating wall, bottom
5,5a	2124	Top block of the film, in-between the LP pads	Solid wall, top Interface, bottom
	2124	Bottom block of the film, in-between the LP pads, directly above the rotor, 5a is contiguous with 5	Interface, top Rotating wall, bottom
6,7,8	2349	Top block of the film, in-between the HP fingers' feet	Solid wall, top Interface, bottom
	324	Middle block of the film, in-between the HP fingers' feet	Interface, top Interface, bottom
	324	Bottom block of the film, in-between the HP fingers' feet, directly above the rotor 6,7 and 8 are contiguous between themselves	Interface, top Rotating wall, bottom
9	1404	Single block of film between the rotor and the HP finger pad-less foot	Solid wall top, Rotating wall bottom

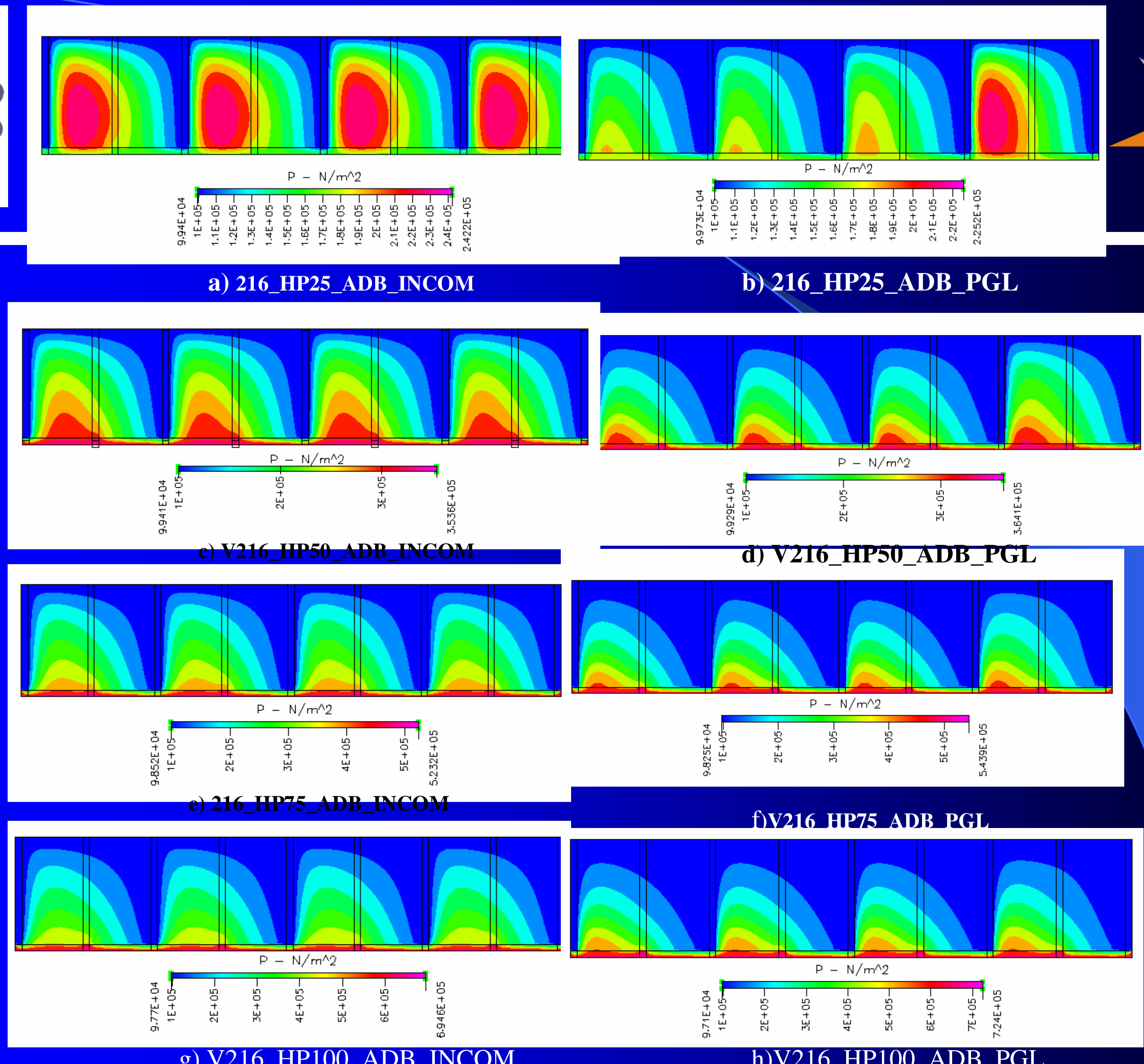

Figure 10. Flow Patterns Under The Finger Seal For Adiabatic Incompressible And Adiabatic Compressible Regimes

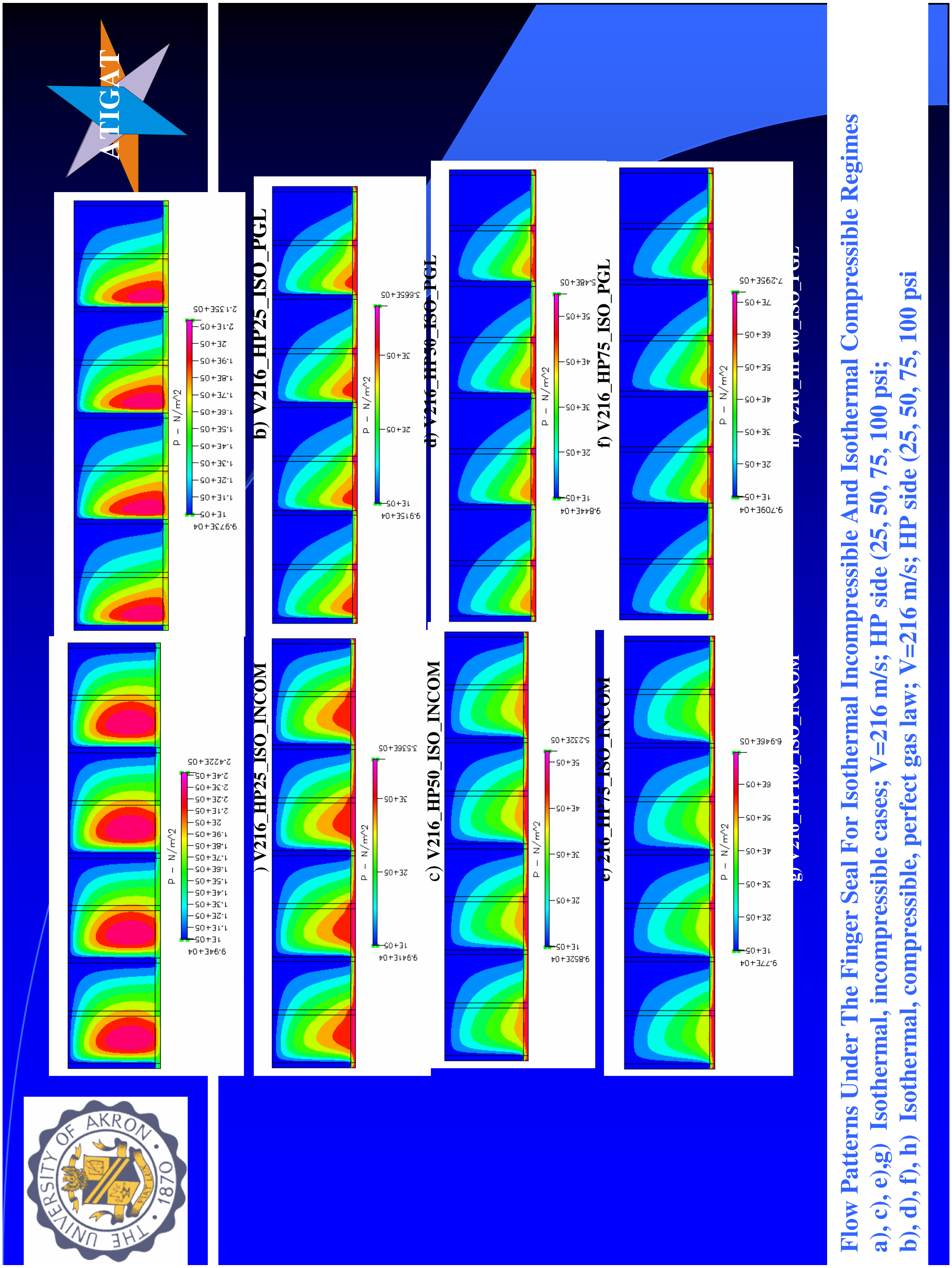
ATIGAT
Flow Patterns Under The Finger Seal For Isothermal Incompressible And Isothermal Compressible Regimes
a), c), e),g) Isothermal, incompressible cases; V=216 m/s; HP side (25, 50, 75, 100 psi;
b), d), f), h) Isothermal, compressible, perfect gas law; V=216 m/s; HP side (25, 50, 75, 100 psi
b) V216_HP25_ISO_PGL
) V216_HP25_ISO_INCOM
c) V216_HP50_ISO_INCOM
f) V216_HP75_ISO_PGL
P - N/m^2
THE UNIVERSITY OF AKRON 1870

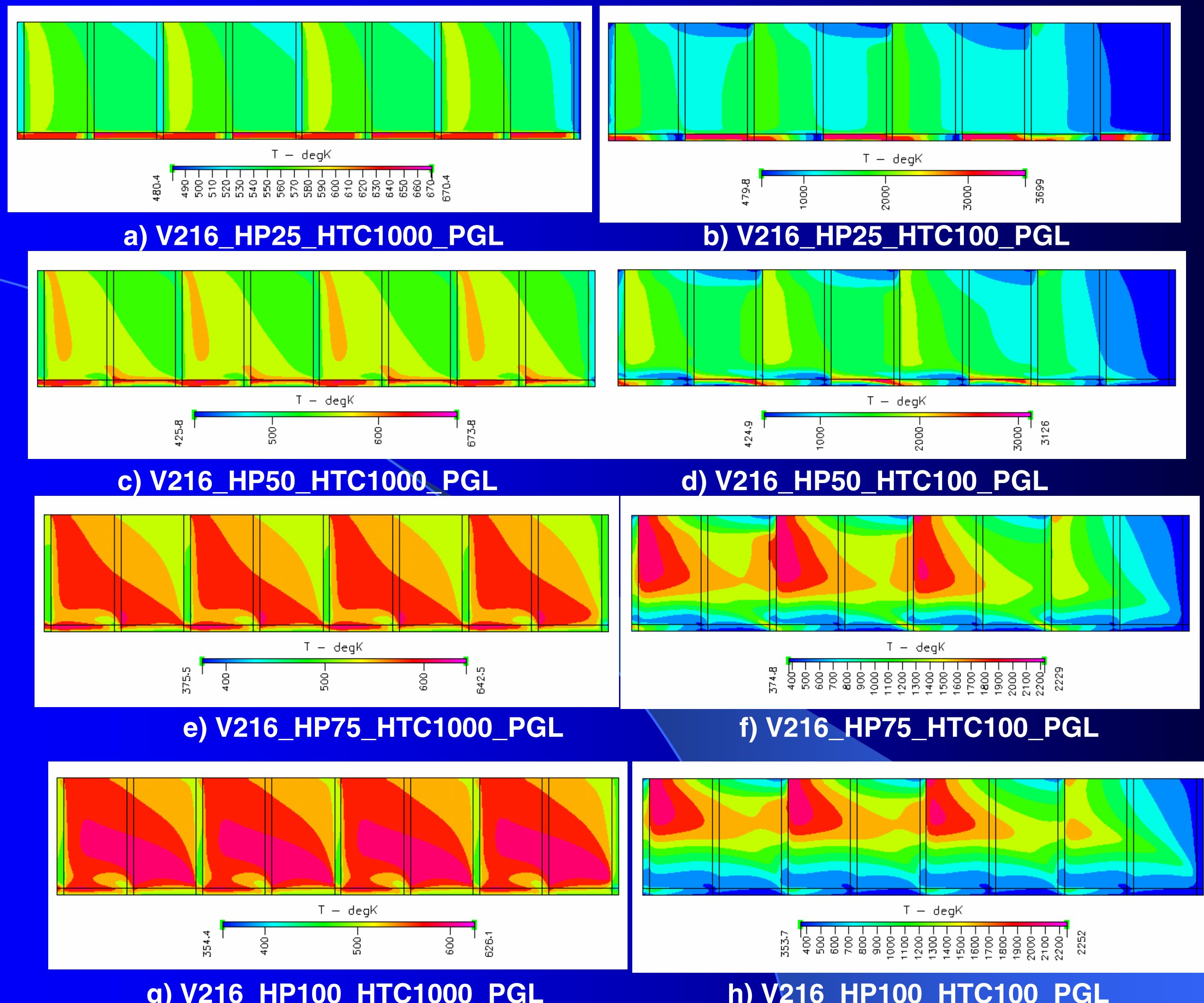

Temperature Patterns Under The Finger Seal when both Density and viscosity vary

a), c), e),g) PGL, with heat transfer coefficient of 1000 W/m^2K; V=216 m/s; HP side (25, 50, 75, 100 psi;
b), d), f), h) PGL, with heat transfer coefficient of 100 W/m^2K; V=216 m/s; HP side (25, 50, 75, 100 psi

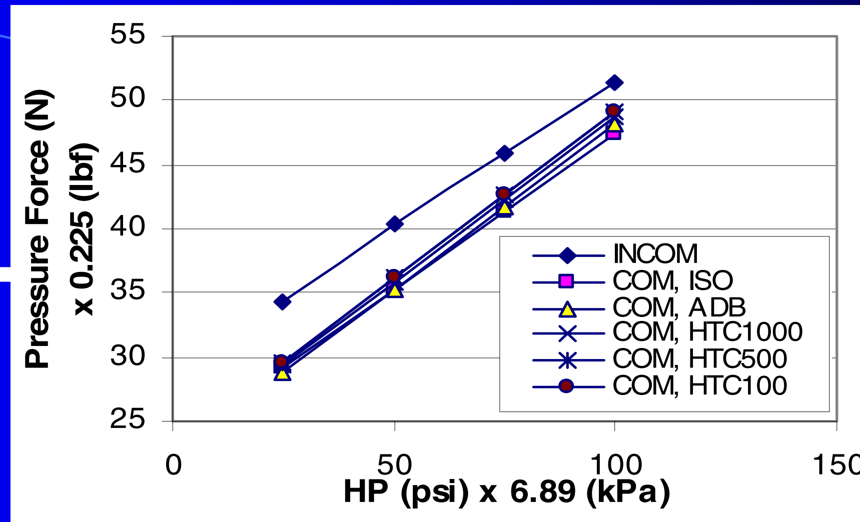

(a)

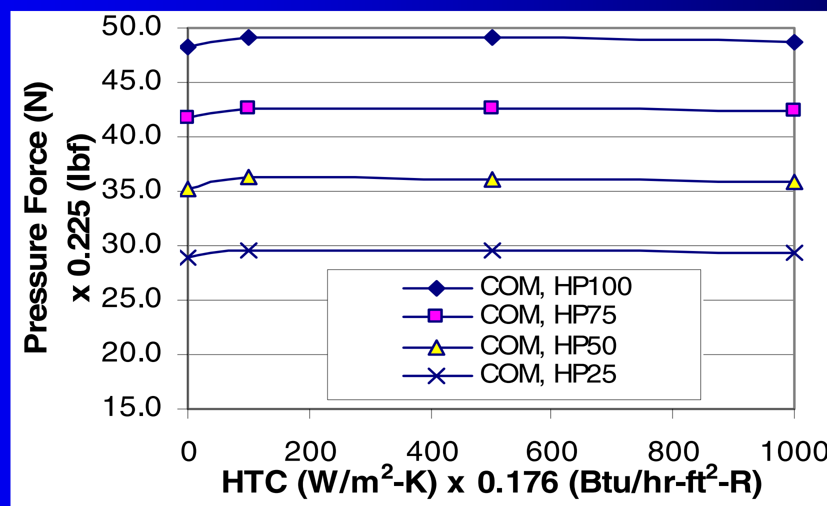

(b)

A Parametric Study of Lifting forces Generated under the 4 HP-4LP pads assembly.

a) **Force variation versus variation of HP side pressure**

b) **b) Force variation versus the heat transfer coefficient when the HP side is varied parametrically**

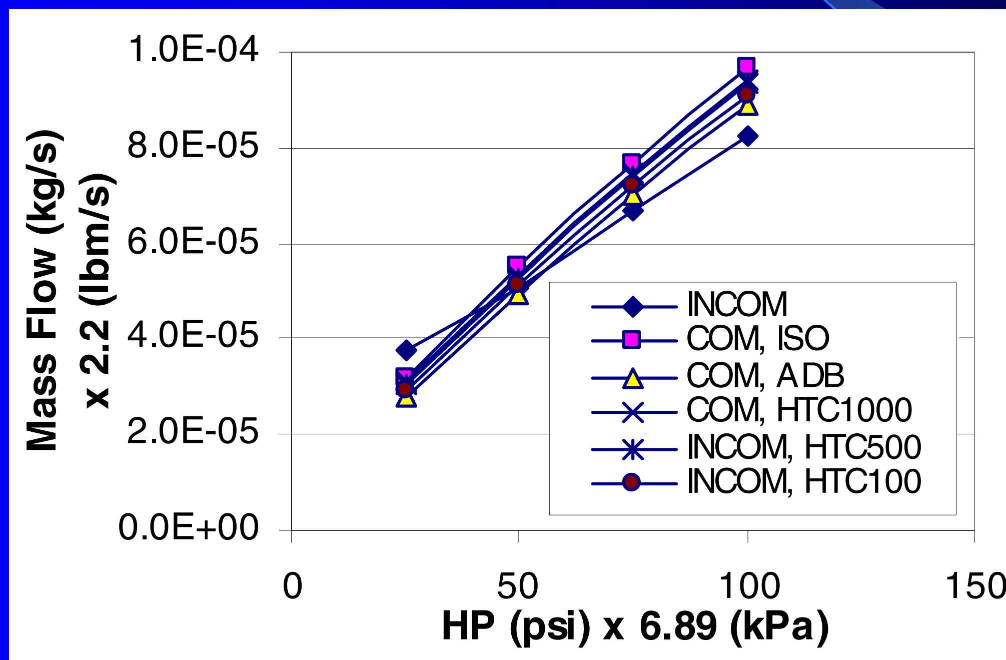

Mass Flow as a Function of the HP side Pressure

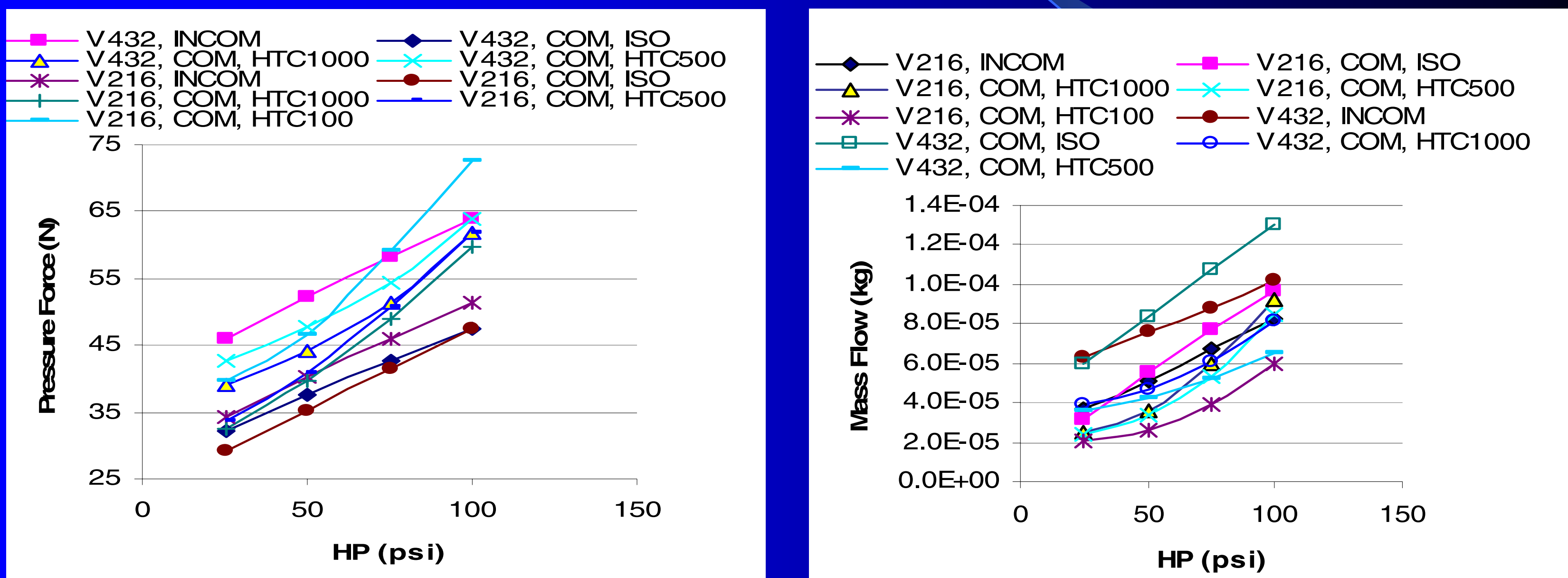

A Parametric Study of Lifting Forces and Mass Flows as a Function of the HP side and Thermal Boundary Conditions when Viscosity is allowed to vary

PARTIAL CONCLUSIONS

ATIGAT

It was found that:

- the interplay between the rotation induced pressure generation and the axial pressure drops controlled by the HP side, is dominated by rotation at low HP side pressure, but it is then taken over by the axial pressure drop when the latter becomes larger then 173kPa at 216mps.
- the effect of allowing the dynamic viscosity to vary with temperature is to introduce strong non-linearities both in the behavior of the leakage flow and the load carrying capability.

PARTIAL CONCLUSIONS

- the numerical experiments showed that the FS behaves more like a bearing at low axial ΔPs and like a seal at high ones
- that the increase in the rotational velocity causes increased LCC, but
- the increase in the heat transfer coefficient causes more leakage and diminishes the load carrying capability.
- that the temperature maps showed that the high temperature regions shift from under the HP fingers at low ΔPs and towards the outer regions of the LP finger pad when the axial ΔPs increase

DYNAMIC SIMULATION CONCEPTS AND RESULTS

FINGER SEAL EQUIVALENT MODEL FOR DYNAMIC SIMULATION

ATIGAT

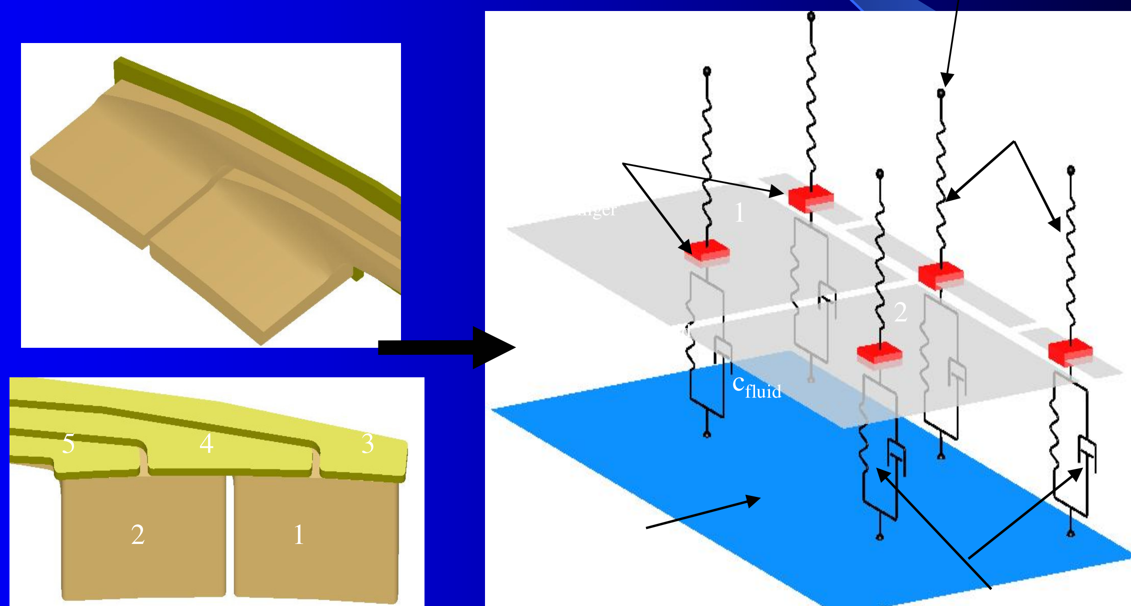

a) b)

Solid model and Equivalent Spring-Mass-Spring/Damper representation for use in the equation of motion simulation

ONE DEGREE OF FREEDOM MODEL

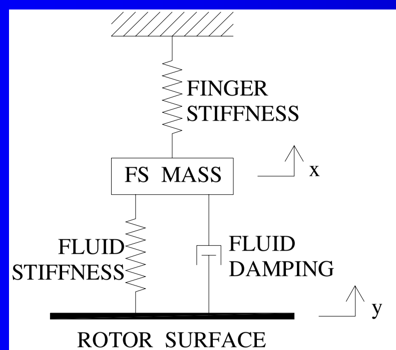

a)

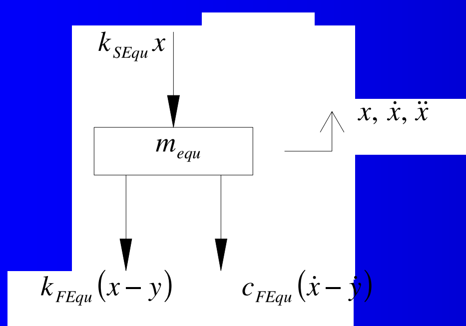

b)

Equivalent Damping and Stiffness Characteristics of the Model Shown in Figure 10

a) Equivalent Spring Dash-pot model

b) Free Body diagram for Derivation of the Equation of Motion

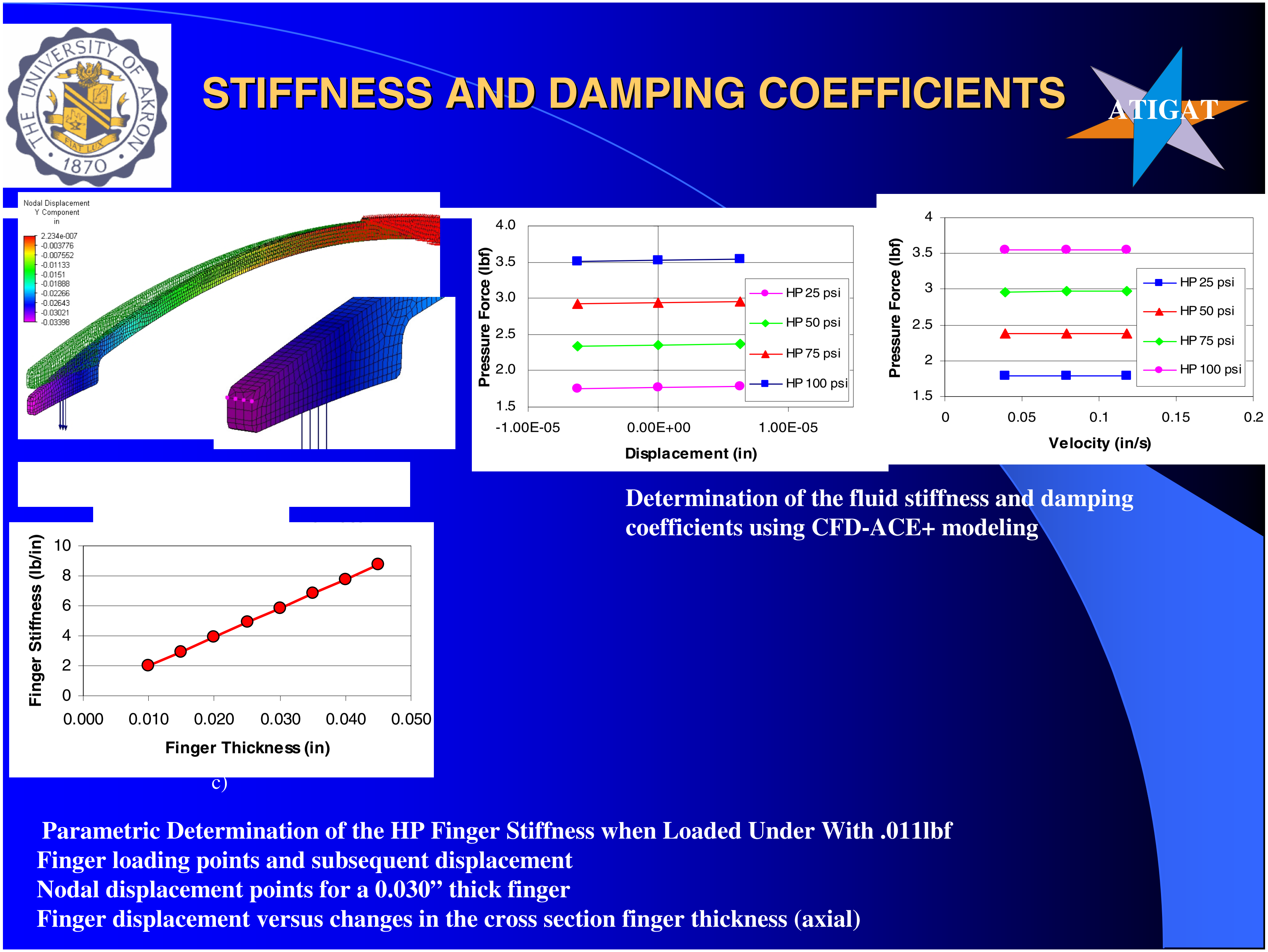
STIFFNESS AND DAMPING COEFFICIENTS
ATIGAT
THE UNIVERSITY OF AKRON 1870
Nodal Displacement
Y Component
in
2.234e-007
-0.003776
-0.007552
-0.01133
-0.0151
-0.01888
-0.02266
-0.02643
-0.03021
-0.03398
Pressure Force (lbf)
Displacement (in)
HP 25 psi
HP 50 psi
HP 75 psi
HP 100 psi
Velocity (in/s)
Finger Stiffness (lb/in)
Finger Thickness (in)
c)
Determination of the fluid stiffness and damping coefficients using CFD-ACE+ modeling
Parametric Determination of the HP Finger Stiffness when Loaded Under With .011lbf
Finger loading points and subsequent displacement
Nodal displacement points for a 0.030" thick finger
Finger displacement versus changes in the cross section finger thickness (axial)

EQUIVALENT STIFFNESS, DAMPING AND FINGERS MASS; THE GOVERNING EQUATION

$$k_{SEqu} = k_{S1} + k_{S2} + k_{S3} + k_{S4} + k_{S5} = 2k_{S1} + 3k_{S3}$$

Solid fingers equivalent stiffness

$$k_{FEqu} = k_{F1} + k_{F2} + k_{F3} + k_{F4} + k_{F5} = 2k_{F1} + k_{F4} + 2k_{F3}$$

Fluid film equivalent stiffness

$$c_{FEqu} = c_{F1} + c_{F2} + c_{F3} + c_{F4} + c_{F5} = 2c_{F1} + c_{F4} + 2c_{F3}$$

Fluid film equivalent damping

$$m_{Equ} = m_{LP1} + m_{LP2} + m_{HP3} + m_{HP4} + m_{HP5} = 2m_{LP1} + 2m_{HP4}$$

Fingers equivalent mass

$$m_{Equ}\ddot{x} + c_{FEqu}\dot{x} + (k_{FEqu} + k_{SEqu})x = c_{FEqu}\dot{y} + k_{FEqu}y$$

Governing Equation

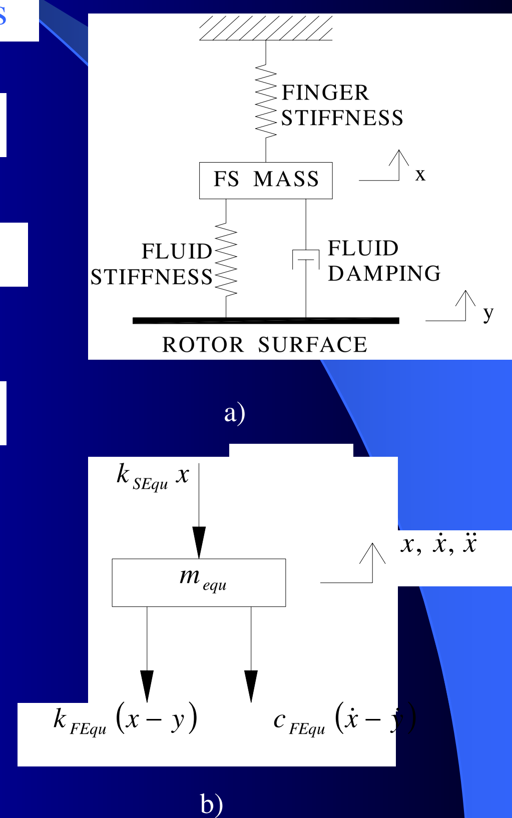

TRANSMISSIBILITY AND PHASE SHIFT

If one applies now a harmonic motion to the rotor surface in the form,

$$y(t) = Y \sin(\omega t)$$

then

$$m_{Equ}\ddot{x} + c_{FEqu}\dot{x} + k_{TEqu}x = $$
$$= k_{FEqu}Y \sin(\omega t) + c_{FEqu}\omega Y \cos(\omega t)$$

And solving for X

$$x_p(t) = X\cos(\omega t - \phi_1 - \phi_2)$$

$$X = Y\left[\frac{k_{FEqu}^2 + (c\omega)^2}{\left(k_{TEqu} - m_{Equ}\omega^2\right)^2 + \left(c_{FEqu}\omega\right)^2}\right]^{1/2}$$

$$\phi_1 = \tan^{-1}\left(\frac{c_{FEqu}\omega}{k_{TEqu} - m_{Equ}\omega^2}\right)$$

$$\phi_2 = \tan^{-1}\left(\frac{k_{FEqu}}{c_{FEqu}\omega}\right)$$

Transmissibility
and
Phase shift

$$T = X/Y$$

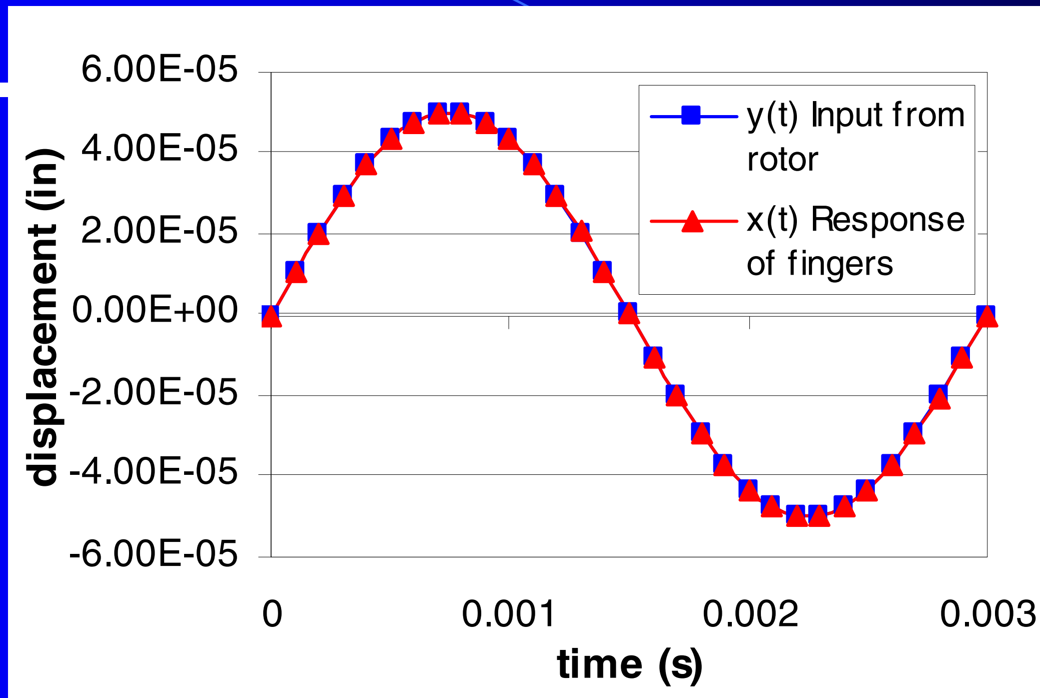

Response of the finger seal model to a harmonic input motion of the rotor.

$$k_{SEqu} = 23.44\frac{\text{lbf}}{\text{in}}(4105\frac{\text{N}}{\text{m}});\ k_{FEqu} = 6852\frac{\text{lbf}}{\text{in}}(6E5\frac{\text{N}}{\text{m}})$$

$$c_{FEqu} = .1\frac{\text{lbf}\cdot\text{s}}{\text{in}}(17.5\frac{\text{N.s}}{\text{m}});$$

$$m_{Equ} = 3.701\text{x}10^{-3}\,\text{lbm}(1.68\text{E}-3\text{kg})$$

$$\boldsymbol{Y} = 5\cdot 10^{-5}\,\boldsymbol{in}(1.27\boldsymbol{E}-3\boldsymbol{mm});$$

$$\omega = 20{,}000\,\boldsymbol{rpm} = 2094\frac{\boldsymbol{rad}}{\boldsymbol{s}};\ \boldsymbol{y}(\boldsymbol{t}) = 5\cdot 10^{-5}\sin(2094\,\boldsymbol{t})$$

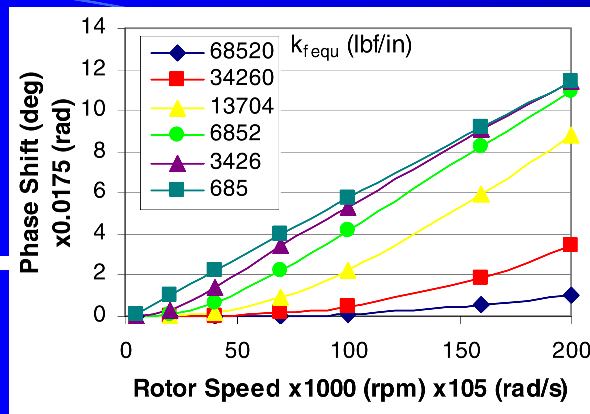

(a)

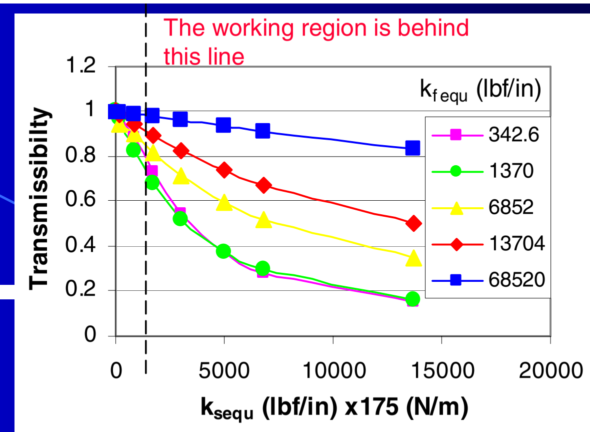

(b)

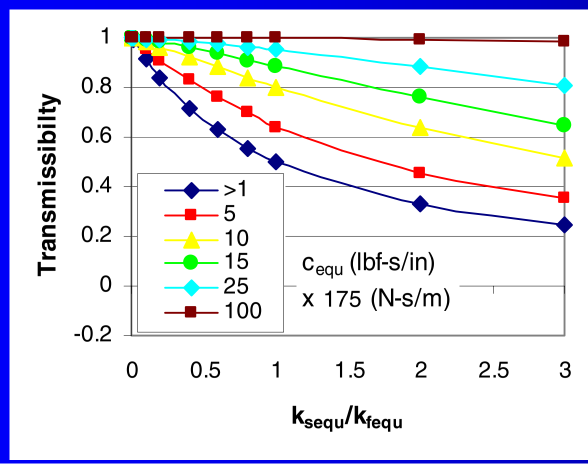

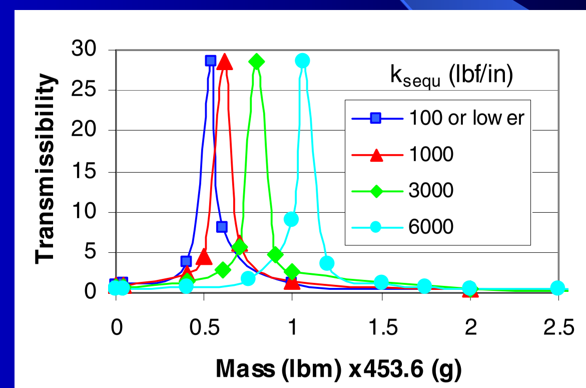

Variations in Displacement Transmissibility and Phase Shift as a Function of the Dynamic System Parameters.

(a) Phase shift of the finger response (ϕ) as a function of the rotor speed for increasing values of the fluid stiffness (kfequ). mequ=0.0037 lbm; ksequ=20.5 lbf/in; cfequ=0.1lbf-s/in.

(b) Transmissibility as a function of the stick stiffness (ksequ) for increasing values of fluid stiffness (kfequ). mequ=0.0037 lbm; cfequ=0.1 lbf-s/in; ω=20,000rpm.

(c) Transmissibility as a function of the stick stiffness/fluid stiffness ratio (ksequ/kfequ) for increasing values of fluid damping (cequ). mequ=0.0037 lbf; ω=20,000rpm.

(d) Transmissibility as a function of the finger mass (mequ) for increasing values of the stick stiffness (ksequ). kfequ=6000 lbf/in; cfequ=0.1 lbf-s/in; ω=20,000rpm

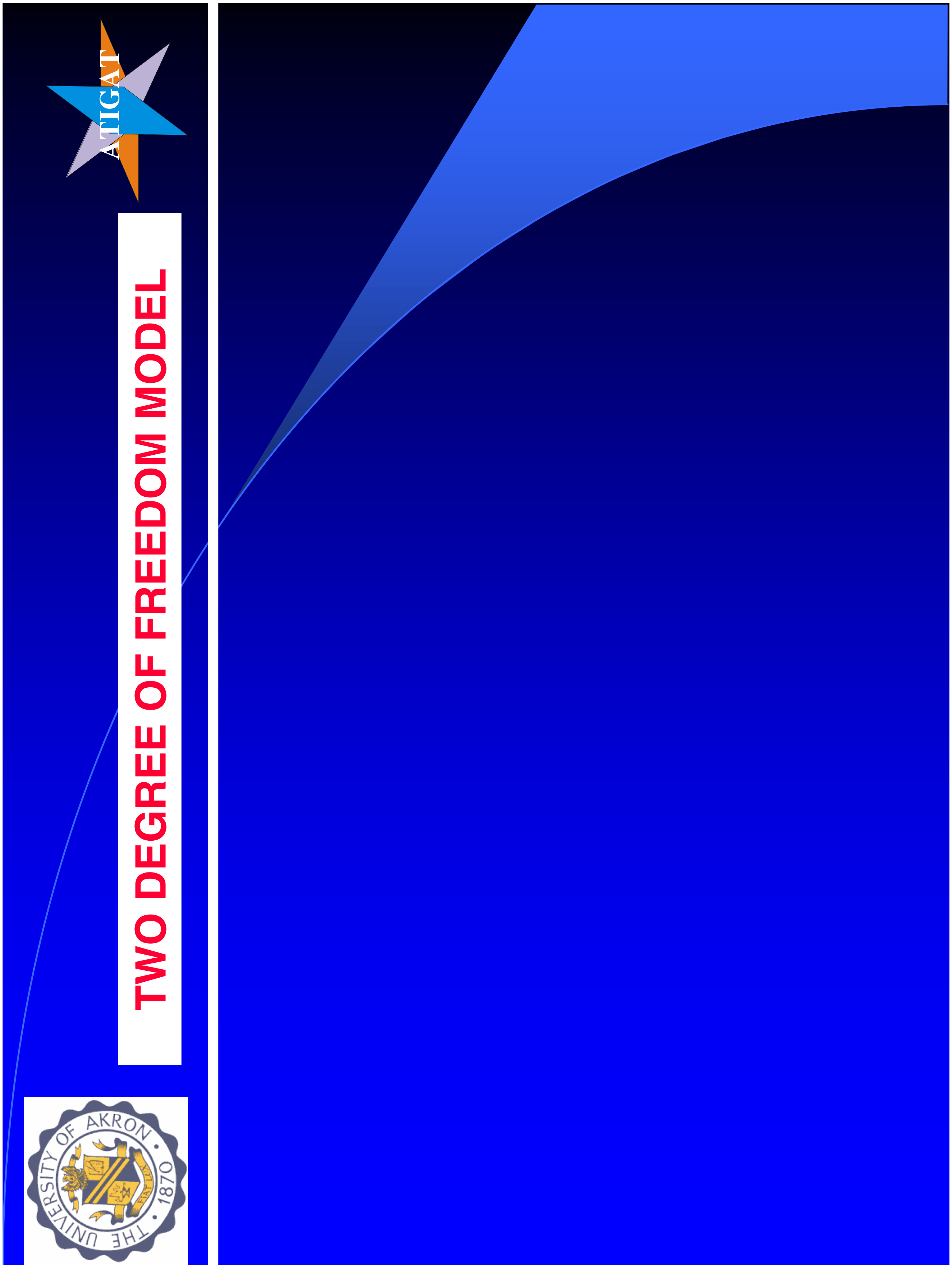
ATIGAT
TWO DEGREE OF FREEDOM MODEL
THE UNIVERSITY OF AKRON
1870

$$\begin{bmatrix} m_R & 0 \\ 0 & m_{FS} \end{bmatrix} \begin{Bmatrix} \ddot{x}_1 \\ \ddot{x}_2 \end{Bmatrix} + \begin{bmatrix} c_f & -c_f \\ -c_f & c_f \end{bmatrix} \begin{Bmatrix} \dot{x}_1 \\ \dot{x}_2 \end{Bmatrix} + \begin{bmatrix} k_f & -k_f \\ -k_f & k_f + k_s \end{bmatrix} \begin{Bmatrix} x_1 \\ x_2 \end{Bmatrix} = \begin{Bmatrix} F_1 \\ 0 \end{Bmatrix}$$

$$x_1(t) = X_1 e^{i\omega t}$$
$$x_2(t) = X_2 e^{i\omega t}$$

$$\begin{bmatrix} Z_{11} & Z_{12} \\ Z_{21} & Z_{22} \end{bmatrix} \begin{Bmatrix} X_1 \\ X_2 \end{Bmatrix} = \begin{Bmatrix} F_0 e^{iwt} \\ 0 \end{Bmatrix}$$

When the Coulomb friction model is activated it replaces the zero right hand side

where

$$Z_{11} = -\omega^2 m_R + i\omega c_f + k_f$$
$$Z_{12} = Z_{21} = -i\omega c_f - k_f$$
$$Z_{22} = -\omega^2 m_{FS} + i\omega c_f + (k_f + k_s)$$

Then the solution is

$$\vec{X} = [Z(i\omega)]^{-1} \vec{F}$$

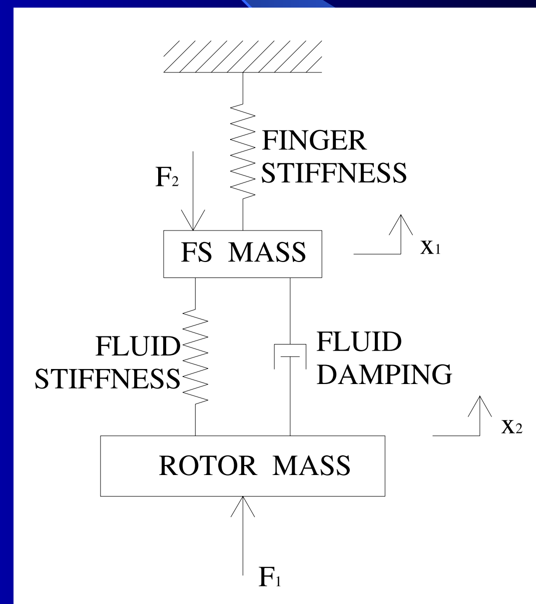

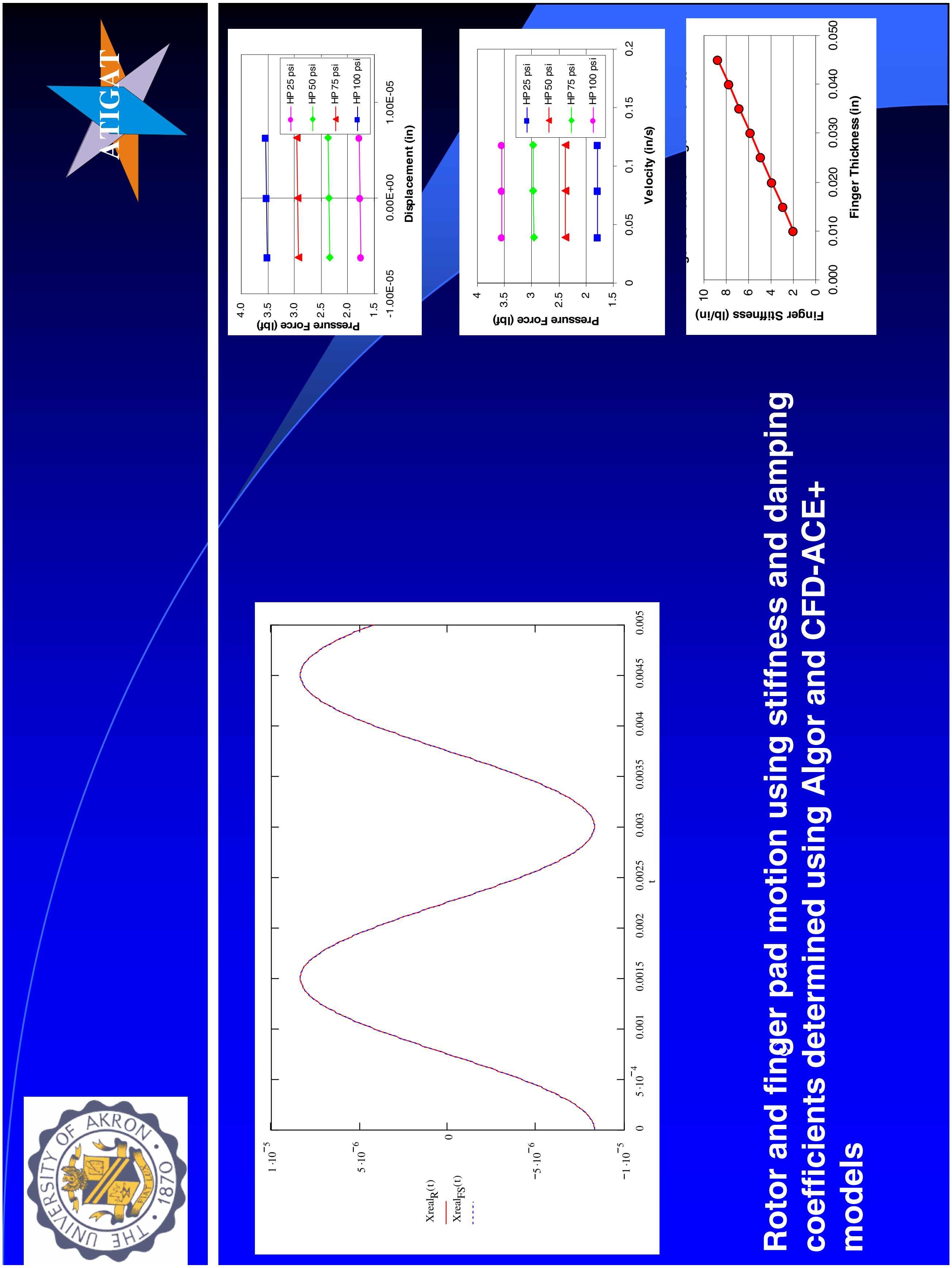
Rotor and finger pad motion using stiffness and damping coefficients determined using Algor and CFD-ACE+ models
ATIGAT
Pressure Force (lbf)
Displacement (in)
HP 25 psi
HP 50 psi
HP 75 psi
HP 100 psi
Velocity (in/s)
Finger Stiffness (lb/in)
Finger Thickness (in)
$Xreal_R(t)$
$Xreal_{FS}(t)$
t

Pad and Rotor motion when the mass of the pad is increased

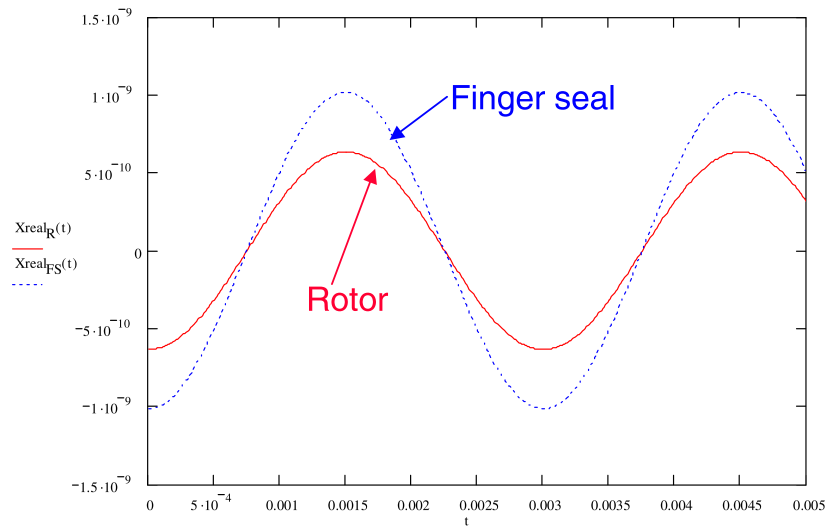

Pad and Rotor motion when the stiffness of the stick is increased

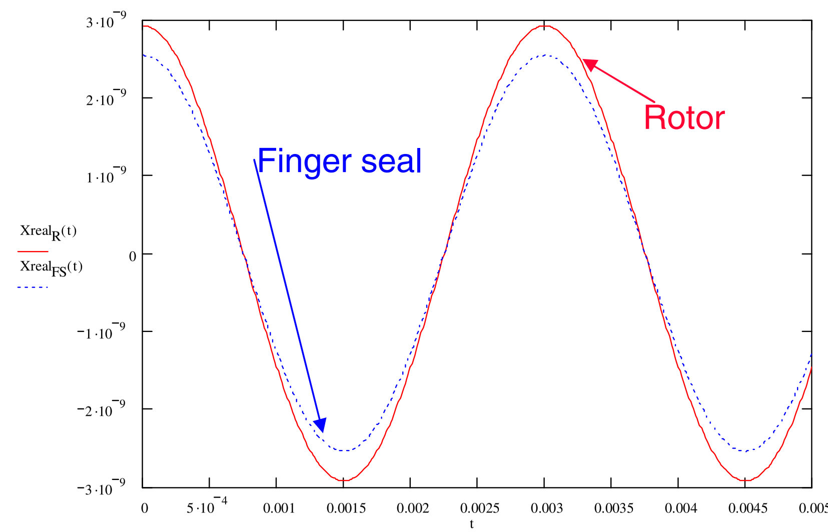

MODEL OF THE ASSEMBLY FOR THE SEAL GLOBAL DYNAMIC COEFFICIENTS

ATIGAT

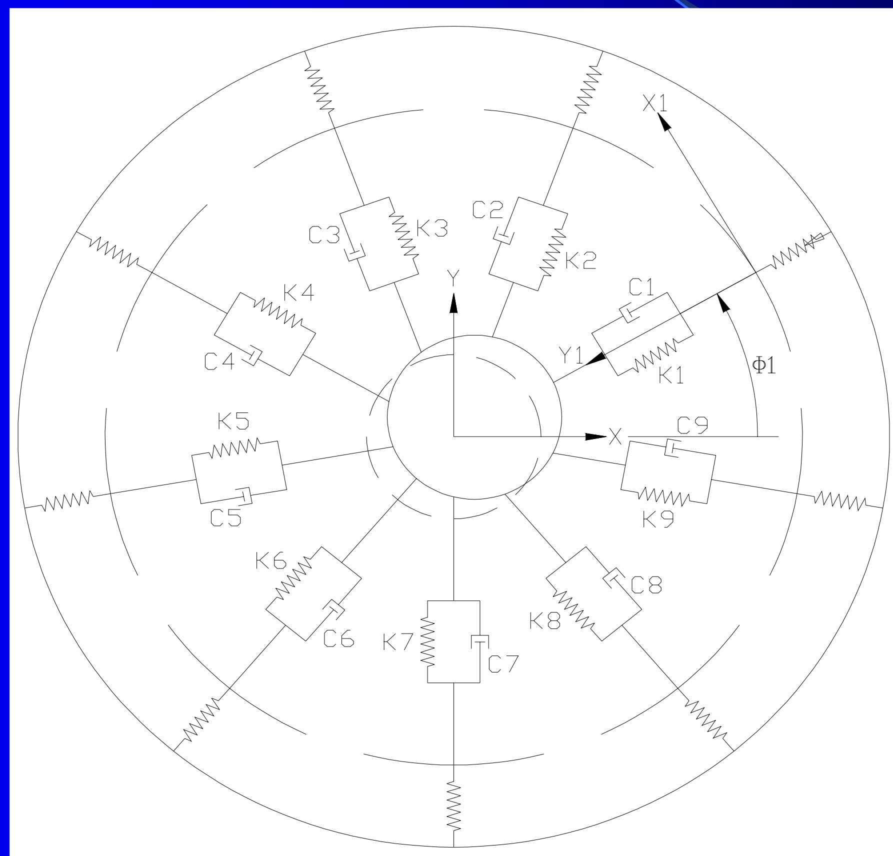

MODEL OF THE ASSEMBLY FOR THE SEAL GLOBAL DYNAMIC COEFFICIENTS

Defining the steady-state equilibrium point of the journal to be the origin for a translated coordinate system

$$(X', Y')$$

the equations of motion for the journal can be written by summing the forces acting on the journal in the

X' and Y'

directions. shows these forces associated with the i^{th} pad, where

F_{ki} = force from i^{th} spring due to a change in rotor position and

F_{ci} = force from i^{th} damper due to a change in rotor velocity.

The forces due to the rotor position and velocity are

$$F_{ki} = K_i y_i'$$
$$F_{ci} = C_i \dot{y}_i'$$

where y_i' and $\dot{y}_i'$ are the radial position and velocity of the journal in i^{th} rotated coordinate system

MODEL OF THE ASSEMBLY FOR THE SEAL GLOBAL DYNAMIC COEFFICIENTS

ATIGAT

Given the position and velocity of the rotor in the (X', Y') coordinate system, it is necessary to perform a coordinate transformation, which yields

$$F_{ci} = C_i(-\dot{X}'\cos\phi_i + \dot{Y}'\sin\phi_i)$$

$$F_{ki} = K_i(-X'\cos\phi_i + Y'\sin\phi_i)$$

Summing forces the differential equation of motion can be written as

$$\delta\dot{x} = A\delta x$$

$$A = \begin{bmatrix} 0 & 0 & 1 & 0 \\ 0 & 0 & 0 & 1 \\ A_{31} & A_{32} & A_{33} & A_{34} \\ A_{41} & A_{42} & A_{43} & A_{44} \end{bmatrix}$$

$$A_{31} = \left(\sum_{i=1}^{9} -K_i\cos^2(\phi_i)\right)/m$$

$$A_{32} = 0$$

$$A_{33} = \left(\sum_{i=1}^{9} -C_i\cos^2(\phi_i)\right)/m$$

$$A_{34} = 0$$

$$A_{41} = 0$$

$$A_{42} = \left(\sum_{i=1}^{9} -K_i\sin^2(\phi_i)\right)/m$$

$$A_{43} = 0$$

$$A_{44} = \left(\sum_{i=1}^{9} -C_i\sin^2(\phi_i)\right)/m$$

$$K_{xx} = -A_{31}$$
$$K_{yy} = -A_{42}$$
$$C_{xx} = -A_{33}$$
$$C_{yy} = -A_{44}$$

THE TEST SECTION ASSEMBLY

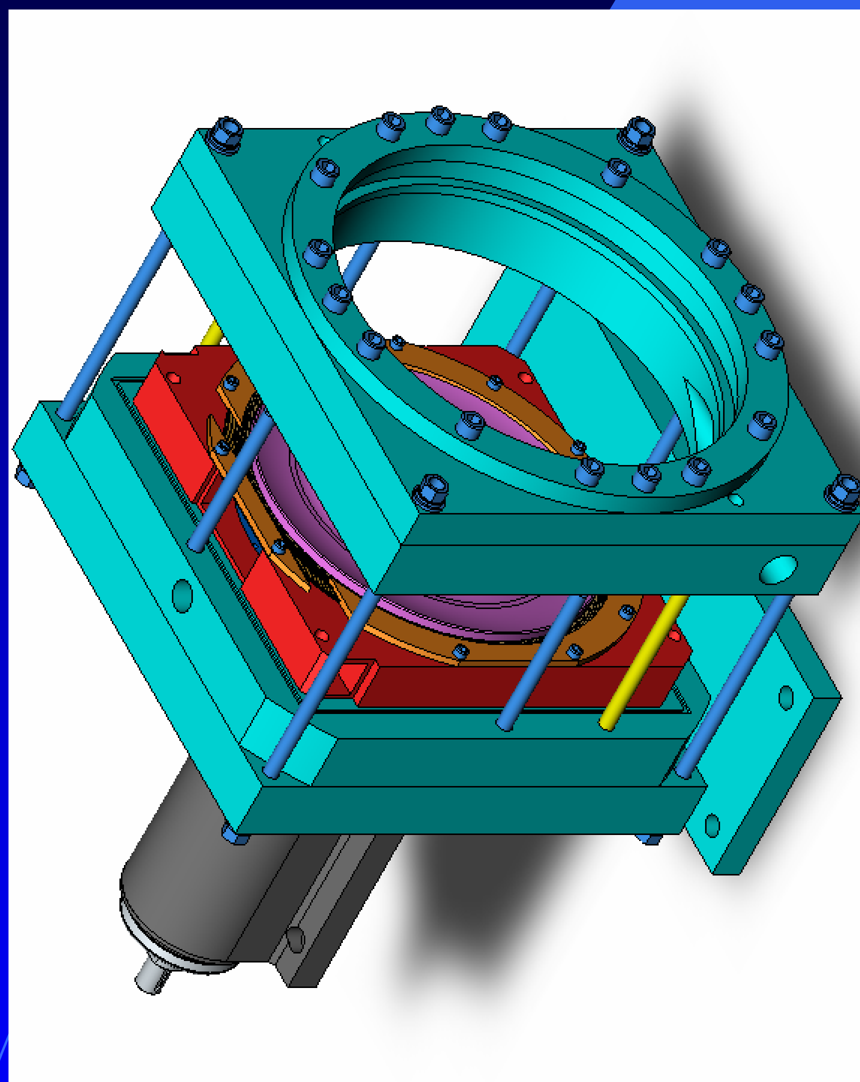

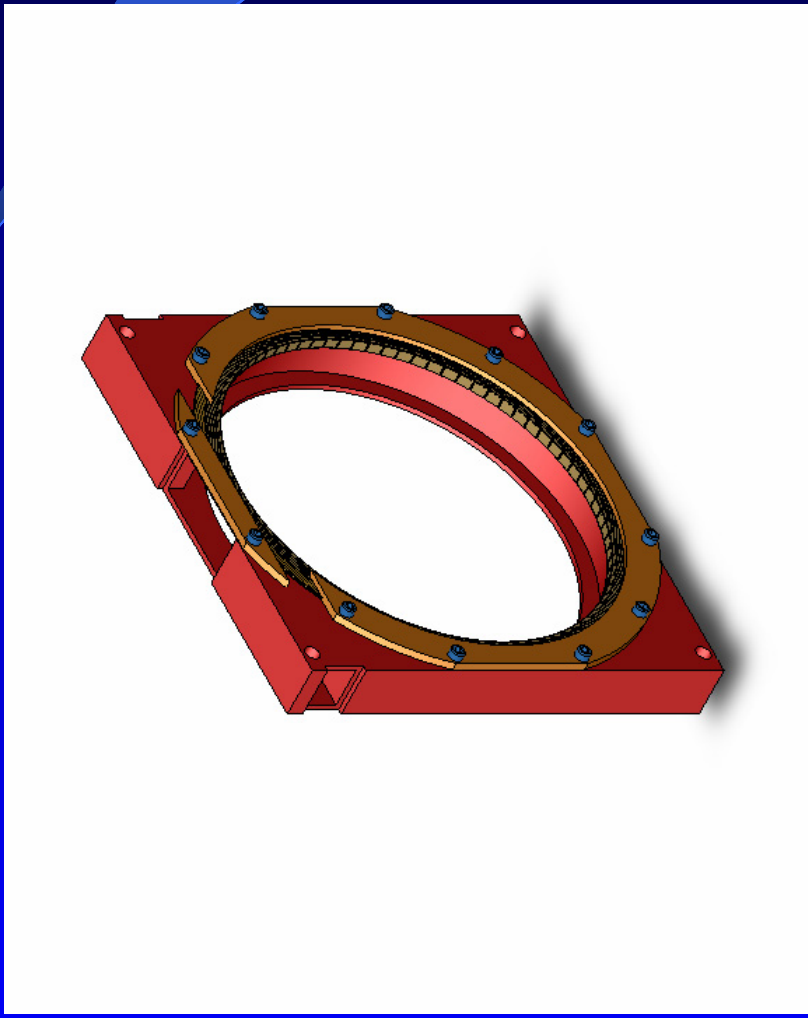

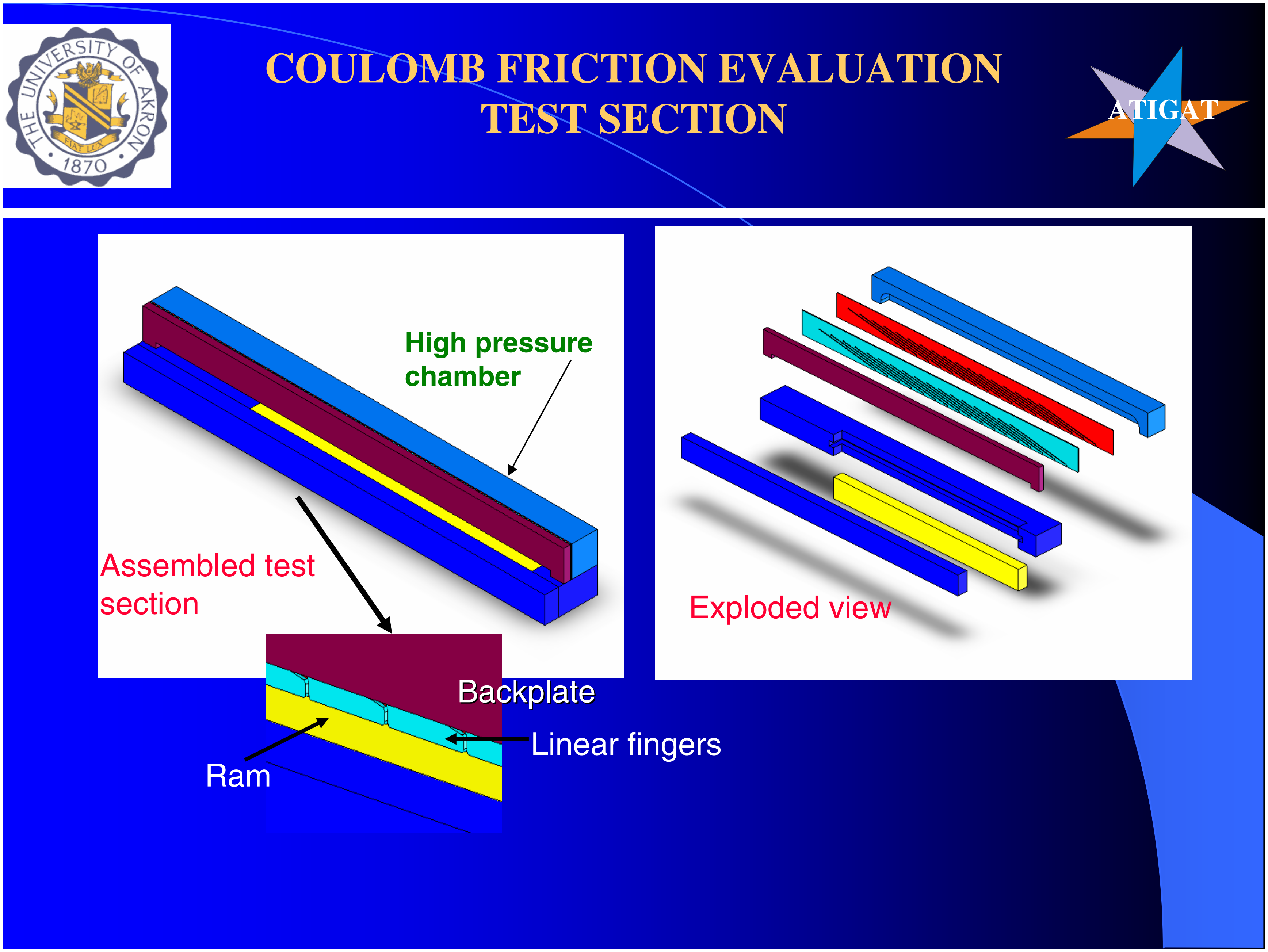
COULOMB FRICTION EVALUATION
TEST SECTION
ATIGAT
High pressure chamber
Assembled test section
Exploded view
Backplate
Linear fingers
Ram

CONCLUSIONS

A three dimensional Navier-Stokes based code (CFD-ACE+/FEMSTRESS) was utilized to analyze the thermofluid behavior of a modified FS[1].

- The pressure patterns, mass flows and load carrying capabilities of this structure were assessed. It was found that even at a lower linear velocity of 216mps (708 fps) the geometry proposed has good lifting capability.

CONCLUSIONS (cont'd)

ATIGAT

- The interplay between the rotation induced pressure generation and the axial pressure drops controlled by the HP side, is dominated by rotation at low HP side pressure, but it is then taken over by the axial pressure drop when the latter becomes larger then 173kPa at 216mps.

- The pressure patterns generated by this geometry at low pressure drops prove that the seal behaves in the fashion of a mini-slider bearing.

CONCLUSIONS (cont'd)

The dynamic model introduced a simplified spring-mass-damper equivalent to the complicated structure presented by the FS.

The numerical experiments concentrated on the determination of the phase shift and displacement transmissibility Y.

These two parameters indicate how well and under what conditions the finger will follow the rotor.

CONCLUSIONS (cont'd)

It was found that

(i) the phase shift values increased when fluid stiffness was low and comparable to that of the stick,

(ii) the phase shift value decreases with fluid damping increase,

(iii) the combination of small *k*SEqu and large *k*FEqu amounts to a transmissibility Y=1,and a reversal in role leads to very small Ys,

(iv) for damping values lower than 175 N.s/m2 (1 lbf.s/in2) damping has no effect on Y and

CONCLUSIONS (cont'd)

ATIGAT

(v) certain combinations of mass and fluid and solid stiffness lead to very large Y when the rotor speed approaches the natural frequency of the system.